JGR Planets

RESEARCH ARTICLE

10.1029/2025JE009631

Rover-Induced Mineral Transformations: Extent of the Effect for the Mars Science Laboratory and Opportunities for Future Landed Mission

J. M. Meusburger[1], T. F. Bristow[1], D. T. Vaniman[2], E. B. Rampe[3], S. J. Chipera[2], D. F. Blake[1], S. L. Simpson[4], R. Y. Sheppard[2,5], and G. Berlanga[6,7]

[1]Exobiology Branch, NASA Ames Research Center, Moffet Field, CA, USA, [2]Planetary Science Institute, Tucson, AZ, USA, [3]Astromaterials Research and Exploration Science Division, NASA Johnson Space Center, Houston, TX, USA, [4]Texas State University - Amentum JETS II Contract at NASA Johnson Space Center, Houston, TX, USA, [5]Institut d'Astrophysique Spatiale, Université Paris-Saclay, CNRS, Orsay, France, [6]BMSIS at NASA Ames Research Center, Moffet Field, CA, USA, [7]Earth and Planetary Sciences Department, UC Santa Cruz, Santa Cruz, CA, USA

Key Points:

- Several highly hydrated minerals rapidly transform under Curiosity-like conditions and are unstable at Martian noon
- Amorphous sulfate phases likely formed on the Martian surface prior to Curiosity sampling and analysis
- Increasing humidity triggers recrystallization of amorphous salt hydrates and may enable their detailed analysis on future Mars missions

Supporting Information:

Supporting Information may be found in the online version of this article.

Correspondence to:

J. M. Meusburger,
johannes.meusburger@gmail.com

Citation:

Meusburger, J. M., Bristow, T. F., Vaniman, D. T., Rampe, E. B., Chipera, S. J., Blake, D. F., et al. (2026). Rover-induced mineral transformations: Extent of the effect for the Mars science laboratory and opportunities for future landed mission. *Journal of Geophysical Research: Planets*, *131*, e2025JE009631. https://doi.org/10.1029/2025JE009631

Received 22 DEC 2025
Accepted 18 FEB 2026

Author Contributions:

Conceptualization: J. M. Meusburger, T. F. Bristow
Formal analysis: J. M. Meusburger, D. T. Vaniman
Funding acquisition: J. M. Meusburger, T. F. Bristow
Investigation: J. M. Meusburger, T. F. Bristow, D. T. Vaniman, E. B. Rampe, S. J. Chipera, D. F. Blake, S. L. Simpson, R. Y. Sheppard, G. Berlanga
Methodology: J. M. Meusburger
Resources: T. F. Bristow
Supervision: T. F. Bristow

Abstract X-ray amorphous sulfate hydrates are a substantial component (up to 23 wt%) of the sedimentary rocks and sands analyzed to date by the Mars Science Laboratory Curiosity rover at Gale crater. Recently, the CheMin X-ray diffractometer observed the amorphization of the crystalline sulfate starkeyite ($MgSO_4 \cdot 4H_2O$) upon exposure to the dry and relatively warm atmosphere inside the rover body. To assess the extent to which interactions between minerals and the rover environment contribute to the amorphous component, we investigated the stability of several hydrated minerals under Curiosity-like conditions. Our results show that highly hydrated minerals are more prone to transformation inside the rover than lower hydrates. Minerals that readily become amorphous under rover conditions are also likely to be unstable when exposed to the dry Martian atmosphere during the warm periods at noon. We therefore suggest that much of the observed amorphization occurred at the Martian surface prior to sampling. Future missions such as the Rosalind Franklin rover and Mars Life Explorer propose to drill into the substantially colder subsurface at Martian mid-latitudes and are likely to encounter temperature and humidity-sensitive cryohydrates. To evaluate the original mineral assemblage of rocks on such missions, it will be critical to maintain controlled temperature and relative humidity (RH) conditions inside the rover body. We find that increasing ambient humidity may induce the recrystallization of amorphous salt hydrates, thus controlling RH and temperature inside the rover would significantly enhance the analytical capabilities of a next generation X-ray diffractometer on Mars.

Plain Language Summary Rocks and sands analyzed by the Curiosity rover at Gale crater on Mars contain large amounts of X-ray amorphous material. In contrast to crystals, X-ray amorphous materials do not produce sharp diffraction peaks and are therefore challenging to analyze for the Curiosity rover. Some sulfate crystals were recently observed to turn X-ray amorphous when exposed to the warm, dry air inside the rover. We tested whether these changes were caused by the rover environment or on the Martian surface. Our results show that highly hydrated minerals are especially sensitive to dry and warm conditions and can readily become amorphous. Minerals that transform inside the rover are also likely unstable on the Martian surface during warm midday periods, suggesting that much of the amorphous material formed before sampling. Future missions will study colder subsurface materials that may be even more sensitive to temperature and humidity. Carefully controlling these conditions inside future rovers could not only preserve delicate minerals but also recrystallize X-ray amorphous salts, thus enabling their detailed characterization by rover instruments. Since hydrated salts are key markers for aqueous environments, this would in turn allow to better understand the environmental conditions present on early Mars.

1. Introduction

Hydrated minerals have been discovered across the Martian surface via orbital spectroscopy and ground-based measurements. From orbit, smectite, hydrated sulfates, and opaline silica are common, especially in some of the most ancient terrains that date to >3 Gyr old (Bishop et al., 2025; Carter et al., 2023). On the ground, the Mars Exploration Rovers identified opaline silica in the Gusev crater (Squyres et al., 2008) and Fe-, Mg-, and Ca-sulfates in the Meridiani Planum (Christensen et al., 2004). Curiosity identified opaline silica, smectite, Fe-, Ca-, and Mg-sulfates, and chlorides (Bristow et al., 2021; Chipera et al., 2023; Rampe et al., 2020; Tutolo

Writing – original draft:
J. M. Meusburger
Writing – review & editing:
T. F. Bristow, D. T. Vaniman, E. B. Rampe, S. J. Chipera, D. F. Blake, S. L. Simpson, R. Y. Sheppard, G. Berlanga

et al., 2025; Vaniman et al., 2018). The Mars 2020 Perseverance rover identified clays (Royer et al., 2024) and Mg and Ca-sulfates (Siljeström et al., 2024). Many hydrated crystalline (mineral) and amorphous phases are sensitive to changes in temperature, relative humidity (RH), and atmospheric pressure (Chipera & Vaniman, 2007; Vaniman et al., 2004). It is therefore critical to understand how Mars-relevant hydrated minerals respond to environmental changes, especially considering that rover-based mineralogical measurements are performed under different environmental conditions than those prevailing in the rock prior to sampling.

The Mars Science Laboratory (MSL) Curiosity rover's Chemistry and Mineralogy (CheMin) and Sample Analysis at Mars (SAM) instruments are housed inside the rover body, where temperatures are substantially warmer (highs up to 35.6°C (Vaniman et al., 2018) than the surrounding atmosphere (typical diurnal range −88 to −13°C; minimum temperature = −102°C; maximum temperature = +20°C (Martínez et al., 2021)). Cold air has a very limited moisture storage capacity. As external air is drawn into the rover body and warmed, the result is extremely low RH conditions (≪1%). In addition, the temperature in the shallow subsurface of Mars bedrock decreases until reaching a steady state equilibrium at a few decimeters of around −53°C (Vaniman & Chipera, 2006). At the typical sampling depth of the Curiosity rover drill (2–6 cm), the temperature generally ranges from about −58 to −13°C and −76 to −45°C in summer and winter, respectively (Martínez et al., 2021). For these reasons, transferring the drilled sample powder into the laboratory instruments inside the rover is always accompanied by an abrupt change in temperature and RH, which may induce phase changes, particularly those that are hydrous.

The CheMin instrument is particularly well-suited for monitoring such changes since sample analysis is non-destructive and can be repeated periodically. The CheMin team recognized the dry humidity conditions as an opportune laboratory for mineral stability experiments on Mars early in the mission.

One experiment involved storing a clay mineral bearing sample called "Cumberland" with a ∼13 Å basal spacing in CheMin for 150 sols (i.e., Martian days) to assess whether it would collapse to 10 Å (Bristow et al., 2015). The mineral remained structurally stable, likely due to partial expansion by metal-hydroxyl groups (Rampe et al., 2025). In contrast, all other smectites in samples analyzed by CheMin from the start of the mission to the Vera Rubin Ridge were fully collapsed, indicating that any originally present hydrated interlayer cations had already been lost before sample delivery and analysis (Rampe et al., 2020).

Another in situ experiment involved monitoring temporal changes in the abundance of the calcium sulfate hydrates gypsum ($CaSO_4 \cdot 2H_2O$) and bassanite ($CaSO_4 \cdot 0.5H_2O$). Vaniman et al. (2018) documented the transformation of gypsum to bassanite within the CheMin instrument within ∼5–15 sols in samples that have <5% gypsum. An exceptional drill sample of a vein with 18% gypsum showed complete dehydration in ∼40 sols (Vaniman et al., 2024). However, because the dehydration of gypsum proceeds slowly relative to CheMin's data acquisition timescale (1–3 sols), and the critical first night of analysis shows no bassanite formation, this transformation is not a significant concern for the instrument's mineral detection capabilities. Even more so, since both the parent (gypsum) and daughter (bassanite) phases remain observable by X-ray diffraction (XRD).

More recently, the complete amorphization of the mineral starkeyite ($MgSO_4 \cdot 4H_2O$) was observed inside CheMin within just three sols (Chipera et al., 2023). While sluggish reactions to other crystalline forms are less problematic, as the daughter phase may still be analyzed, amorphization is associated with the loss of long-range order, thus the transformation product does not produce discrete Bragg peaks and only contributes to the background scattering. In a comprehensive study of the response of various Mg-sulfate and Ca-sulfate hydrates to the dry conditions under low atmospheric pressure prevailing on contemporary Mars, Chipera and Vaniman (2007) observed amorphization of other $MgSO_4$ hydrates such as epsomite ($MgSO_4 \cdot 7H_2O$) and hexahydrite ($MgSO_4 \cdot 6H_2O$) within hours under low-RH and atmospheric pressure conditions. They hypothesize that the formation of the amorphous $MgSO_4$ hydrate phase is probably induced by the rapid dehydration, with kinetics inhibiting the formation of thermodynamically favored crystalline phases. Many other salt minerals exhibit a high-water content, rendering them susceptible to rapid dehydration or amorphization inside CheMin or any other rover/lander-hosted analytical instrument.

To gain a thorough understanding of the temperature conditions inside the CheMin instrument, we review thermocouple data for each of the drill campaigns up to "Kings Canyon" (sol 4266). Based on these data, we then determine whether low RH and atmospheric pressure-induced amorphization extend beyond $MgSO_4$ to other geochemically relevant systems including $FeSO_4$–H_2O and $MgCl_2$–H_2O. This will provide critical insights into

the likely components making up amorphous materials in Gale crater samples and the extent of amorphization occurring inside the Curiosity rover body.

Another objective is to assess the requirements for the environmental conditions inside future spacecraft, such as the ExoMars Rosalind Franklin and Mars Life Explorer landers, aiming to search for signs of current life in the Martian subsurface (Vago et al., 2017; Williams et al., 2023). Lastly, potential advantages for a controlled temperature and humidity reaction environment for future landed missions on Mars will be explored.

2. Materials and Methods

2.1. Temperature Conditions Inside the CheMin Instrument

Temperature conditions inside the CheMin instrument were monitored using three platinum resistance thermometers: Therm-2615, located at the baseplate of the CheMin CCD detector; Therm-2617, on the CheMin power board; and Therm-2632, at the interface where the instrument is bolted. The temperature measured by Therm-2617 at the power board increases once a measurement starts (Chipera et al., 2023); therefore, Therm-2615 was used instead, as it more accurately represents the temperatures experienced by the sample. Therm-2615 data from each of the first 45 sampling campaigns up to and including sol 4266 (i.e., the end of the Kings Canyon drill campaign), were used to calculate: (a) Tmax, the maximum temperature across all analysis sols; (b) Tmin, the minimum temperature across all analysis sols; and (c) Tav, the average temperature across all analysis sols.

2.2. Synthesis and Identification of Starting Phases

We have found that highly hydrated reagents can be prone to partial dehydration upon exposure to dry laboratory atmospheres, for example, when their storage containers are opened to retrieve the reagent for experiments. Therefore, epsomite ($MgSO_4 \cdot 7H_2O$) and melanterite ($FeSO_4 \cdot 7H_2O$) reagent powders were equilibrated in a chamber with saturated NaCl salt solution buffering the RH at 75% (Greenspan, 1977) for at least 30 days before use. This ensured that starting material was exclusively in the heptahydrate state, as confirmed by X-ray diffraction (XRD).

Rozenite and hexahydrite were formed by the dehydration of the respective heptahydrate reagent powders at room temperature (approx. 22°C) in a drier (i.e., 33% RH (Greenspan, 1977)) atmosphere maintained by a saturated $MgCl_2$ solution over 69 and 120 hr, respectively. Starkeyite ($MgSO_4 \cdot 4H_2O$) was formed by the dehydration of fine $MgSO_4 \cdot 7H_2O$ reagent powder at 50°C in $MgCl_2$ humidity-buffered air over 5 days.

Kieserite ($MgSO_4 \cdot H_2O$) was synthesized hydrothermally using an approach similar to Meusburger et al. (2020): 6 g of epsomite reagent powder was dissolved in 22 ml of 73 wt% H_2SO_4, heated at 220°C in a hydrothermal autoclave for 48 hr after which the oven was turned off and the autoclave was left to cool down for 16 hr. The synthesis product was mechanically extracted from the Teflon vessel and washed twice in distilled water taking advantage of the relatively slow dissolution kinetics of kieserite (Karsten, 1954). Finally, the product was washed in ethanol and dried in an oven at 100°C for 1 hour. The final synthesis product contained 94 wt% of kieserite and 6 wt% of hexahydrite, which likely has formed during the washing procedure. We note that this hydrothermal approach was used since dehydrating epsomite powder at high-temperatures often results in the formation of the $MgSO_4$ $1.25H_2O$ phase or mixtures of this phase and kieserite, unless the dehydration is carried out at high relative humidity over a timescale of several weeks (Chipera & Vaniman, 2007).

While szomolnokite may be readily obtained using an analogous hydrothermal approach (Meusburger et al., 2019), we used the much simpler method outlined in Bishop et al. (2025) and dehydrated $FeSO_4 \cdot 7H_2O$ reagent powder over 4 days at 60°C using the $MgCl_2$ humidity-buffer setup, which yielded phase pure szomolnokite powder.

Once synthesized, starkeyite ($MgSO_4 \cdot 4H_2O$), rozenite ($FeSO_4 \cdot 4H_2O$), kieserite ($MgSO_4 \cdot H_2O$), szomolnokite ($FeSO_4 \cdot H_2O$), and bischofite ($MgCl_2 \cdot 6H_2O$) were transferred into a glove box containing K-acetate, buffering the RH at ~22% RH. Epsomite ($MgSO_4 \cdot 7H_2O$) and melanterite ($FeSO_4 \cdot 7H_2O$) were handled in a still air box at a RH of ~80%, whereby the humidity was raised manually using a water spray bottle. Hexahydrite ($MgSO_4 \cdot 6H_2O$) was handled in the ambient laboratory air (~42% RH). All samples were spiked with ZnO and sealed inside an MSE PRO air-sensitive sample holder using a Kapton tape to prevent hydration state changes during analysis. The phase

identity of the starting materials was confirmed by XRD using a Rigaku Smartlab X-ray diffractometer. The diffracted Cu-K$\alpha_{1,2}$ photons were detected using a *D*/teX Ultra 250, a *1D* silicon strip detector. Diffraction patterns were acquired in 5–65° 2θ range with a step size of 0.01° and a scan speed of a maximum 3°/min. The instrument profile parameters were derived from a NIST 640c silicon standard and all Rietveld refinements were performed using the GSAS-II software (Toby & Von Dreele, 2013).

2.3. Simulation of Environmental Conditions Inside the Curiosity Rover

All experiments were conducted either in a double valve Yomato ADP-200C vacuum oven or a double valve vacuum desiccator (Figure S1 in Supporting Information S1). One valve was connected to a Terranova Model 906 Convection Gauge for pressure monitoring, while the other valve was connected to an Agilant Varian dry scroll pump to manually maintain a range of 5.2–7.2 torr, approximating present-day Martian atmospheric pressure conditions (Néri et al., 2020). The ambient laboratory temperature (∼20°C) closely corresponds to the average Therm 2615 temperature inside CheMin (∼13.4°C) and was monitored using a Vaisala temperature probe. For the runs at elevated temperature (40°C), the temperature was monitored using an AMS 8607BLE pressure, temperature and humidity Bluetooth sensor placed inside the oven.

A beaker containing anhydrous $MgCl_2$ was placed inside the desiccator to bind moisture from the released sample and maintain ∼0% RH as confirmed by the AMS 8607BLE Bluetooth sensor. After initial phase identification, the ZnO-spiked samples were placed inside the vacuum chamber. After the end of the experiment, the samples were quickly (∼30 s transfer time) transferred to the K-acetate humidity buffered glove box (22% RH (Greenspan, 1977)) after which the samples were again loaded into Kapton-sealed powder holders for XRD analysis.

It is well established that amorphous $MgSO_4$ hydrate rapidly crystallizes upon exposure to elevated RH under ambient laboratory conditions (Wang et al., 2009). We have carried out experiments to test whether this behavior persists under Martian pressure conditions: Amorphous magnesium and iron sulfate hydrates produced in the previous runs from epsomite and melanterite as well as the AMS 8607BLE Bluetooth sensor were transferred to a vacuum chamber. A Bluetooth connection between the sensor and a smartphone allowed environmental conditions inside the desiccator to be monitored. To increase the humidity, ∼150 mg of water was added to a weighing boat inside the ∼10 L vacuum chamber of the Yomato oven, which should result in a target humidity of ∼82% RH and corresponding target pressure of 20.5 torr. The pressure and humidity at the start of all experiments were 5.2 torr and 0% RH, but rapidly increased in the presence of the water drop (e.g., to 11.5 torr and 32% RH within 15 min of starting the amorphous $MgSO_4$ run). After the experiment was terminated all of the water in the weighing boat had evaporated but the pressure and humidity inside the vacuum chamber were lower than the expected pressure and humidity (e.g., only 13 torr and 40% RH for the amorphous $MgSO_4$ run) indicating that at least some of the water vapor had been taken up by the sample. The temperature remained in the 19–21°C range throughout these experiments. The resulting powders were analyzed by means of XRD.

2.4. Use of AI-Assisted Technolgy

An AI-based language tool (ChatGPT, OpenAI) was used for minor language editing of an early draft. The authors take full responsibility for the manuscript.

3. Results and Discussion

3.1. Conditions Inside CheMin and Sampling Workflow

A typical sample-acquisition workflow begins with drilling into a rock target (or less often scooping unconsolidated sediment). The resulting drill powder or scooped material is then delivered to CheMin by the Sample Acquisition, Sample Processing, and Handling–Collection and Handling for In Situ Martian Rock Analysis (SA/SPaH-CHIMRA) system. At the beginning of the MSL mission, prior to delivery into CheMin, SA/SPaH-CHIMRA would sieve the material to <150 μm to prevent clogging of the analysis cell. This processing chain failed at about sol 1496 of the mission, after which samples were delivered to CheMin by simply positioning the drill over the CheMin sample inlet and back-rotating the drill auger. Fortuitously, the powder thus delivered is consistently fine-grained and performs as well in CheMin XRD as the sieved powder did (Vaniman et al., 2024). Detailed descriptions of the CheMin and SA/SPaH-CHIMRA instruments can be found in Anderson et al. (2012) and Blake et al. (2012, 2024), respectively.

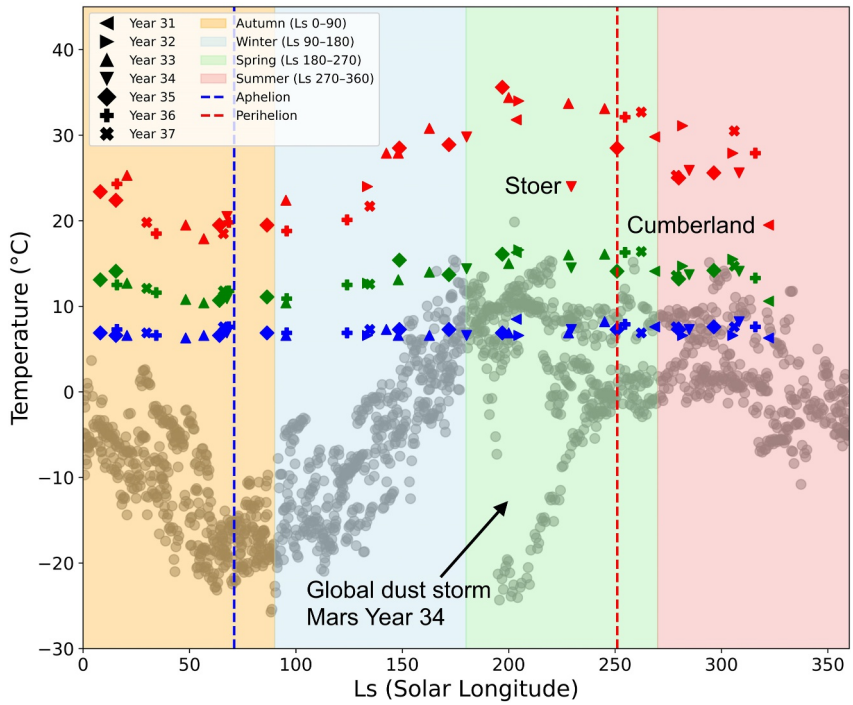

Figure 1. Compilation of the seasonal variation of the maximum (red markers), minimum (blue markers), and average (green markers) temperatures inside CheMin based on interior platinum resistance thermocouple number 2615 data including all drill holes up to "Kings Canyon" (sol 4266). Diurnal maximum ground temperatures for the first 2500 sols reported by Martínez et al. (2021) are plotted as gray circles.

Once the sample resides inside the analysis cell, it is exposed to dry and relatively warm conditions with maximum diurnal temperatures ranging from 17.6 to 35.6°C. The maximum temperature inside CheMin appears to be primarily driven by the surrounding temperature and thus shows strong seasonal variability (Figure 1): Comparison of CheMin temperatures with the diurnal maximum ground temperatures for the first 2500 sols (Martínez et al., 2021) shows that the temperature increase following the aphelion (when Mars farthest from sun) and the subsequent decrease following the perihelion (when Mars closest to sun) are clearly reflected in the maximum CheMin instrument temperatures (Figure 1). The Stoer and Cumberland drill samples show relatively low maximum temperatures because they were acquired during periods of reduced ground temperatures (diurnal temperature maxima of −5.9 and −5.6°C, respectively). Such temperature drops may be caused by dust storms, which are responsible for the pronounced decrease in ground temperatures between Ls = ∼180–250 (Martínez et al., 2021), and during which the Stoer sample was acquired. In contrast, both the average and minimum temperatures within CheMin exhibit far less pronounced seasonal variability (i.e., T_{av} = 10.4–16.6°C; T_{min} = 6.3–8.5°C), likely due to the constant heat flux from Curiosity's Radioisotope Thermoelectric Generator that is being dumped into the rover deck where CheMin is bolted. Because T_{min} remains relatively stable throughout the year, diurnal variations are primarily driven by T_{max} and become strongest when T_{max} is high, as further reflected by the strong correlation ($r = 0.99$) between T_{max} and $\Delta(T_{max} - T_{min})$ (Figure S2 in Supporting Information S1).

3.2. Extent of the Effect for the Mars Science Laboratory

Table 1 summarizes the experimental conditions of each run and the corresponding diffraction data are displayed in Figures 2 and 3. The results are discussed in detail in the following sections.

3.2.1. $MgSO_4$–H_2O System

On exposure to the dry conditions (RH ≈ 0%), at Mars-relevant pressures, epsomite and hexahydrite became completely amorphous within 5 and 7 hr at 20–21°C (Figure 2). This transformation was anticipated, as the low-pressure instability of these minerals has been documented in several previous studies (Furnari et al., 2025;

Table 1
Pressure (torr) and Temperature (°C) Conditions and Duration (D in Hours) During the Experimental Runs and How Each Mineral Responded to These Conditions; wt% (Start) and wt% (End) Correspond to Weight Percent of ZnO

Mineral	Formula	wt% (start)	wt% (end)	Response	*T* (°C)	*D* (h)	P (torr)
Epsomite	$MgSO_4 \cdot 7H_2O$	35.2	100	Amorphization	20	5	5.2–5.4
Hexahydrite	$MgSO_4 \cdot 6H_2O$	33.1	100	Amorphization	21	7	5.2–5.5
Starkeyite	$MgSO_4 \cdot 4H_2O$	36.7	35.8	Stable	18–21	72	5.2–6.0
Starkeyite	$MgSO_4 \cdot 4H_2O$	39.0	55.0	Amorphization	40	24	5.2–5.7
Kieserite	$MgSO_4 \cdot H_2O$	45.0	45.2	Stable	40	24	5.2–5.6
Melanterite	$FeSO_4 \cdot 7H_2O$	51.2	100	Amorphization	21	4	5.2–5.35
Rozenite	$FeSO_4 \cdot 4H_2O$	53.4	58.5	Amorphization	18–21	72	5.2–8.65
Rozenite	$FeSO_4 \cdot 4H_2O$	41.2	90.4	Amorphization	40	24	5.2–5.6
Szomolnokite	$FeSO_4 \cdot H_2O$	27.5	25.6	Stable	40	24	5.2–5.9
Bischofite	$MgCl_2 \cdot 6H_2O$	23.7	14.5	Dehydryation[a]	19–21	24	5.2–5.7
Bischofite	$MgCl_2 \cdot 6H_2O$	24.5	27.1	Dehydryation[a]	40	24	5.25–6.0

Note. Increase in the ZnO component indicated dehydration or amorphization. Precision error 0.01 wt%, accuracy error of ~3 wt% (Hillier, 2000). [a]Absolute phase fractions not accurate since the unknown phase was not included into the refinement.

Sheppard et al., 2022; Vaniman & Chipera, 2006; Vaniman et al., 2004). 20°C also corresponds to the maximum temperature Curiosity observed within the 2500 mission sols; thus, it is unlikely that hexahydrite and epsomite are stable under the present-day environmental conditions prevailing at Gale crater.

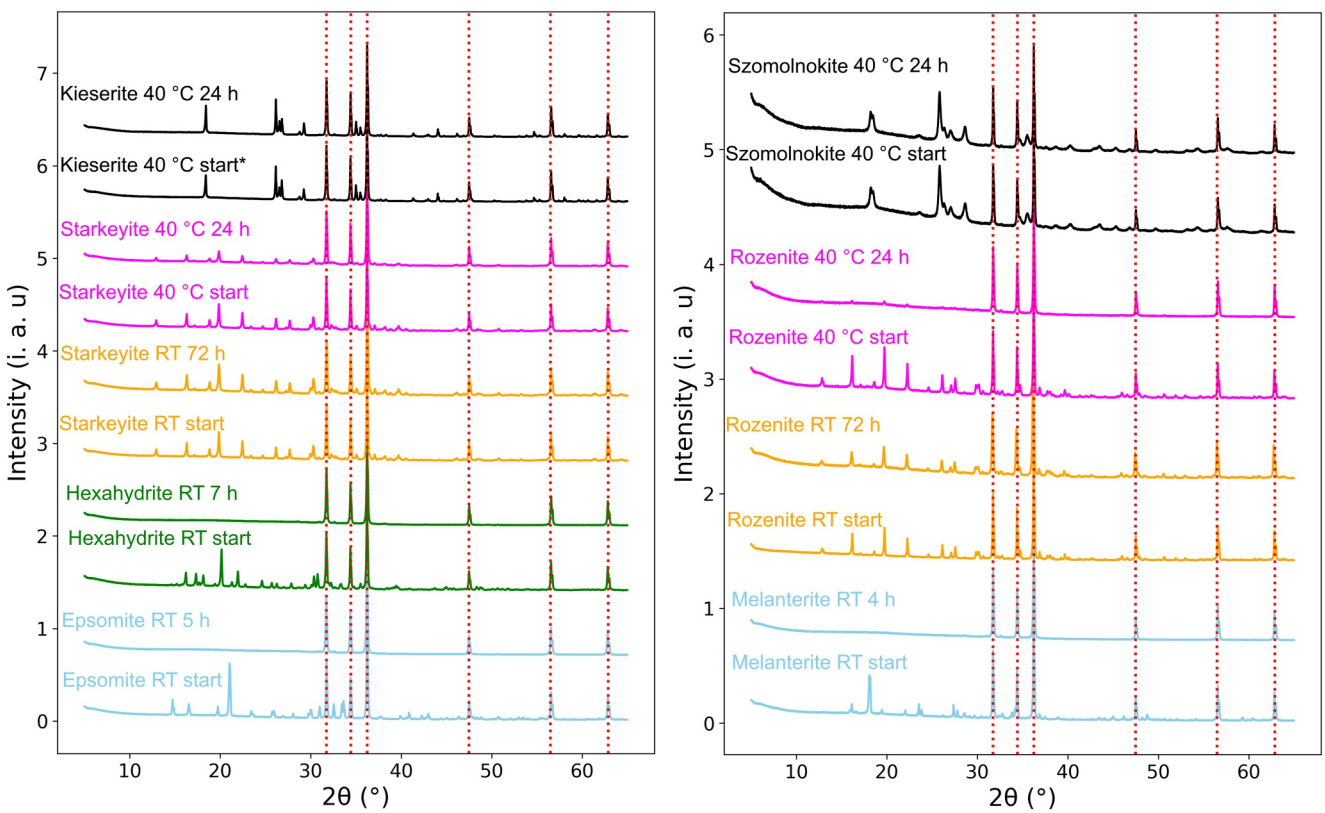

Figure 2. X-ray diffraction patterns acquired at the start and end of the individual runs for (left) magnesium sulfate and (right) iron sulfate hydrates. Dotted vertical red lines mark Bragg peaks originating from the ZnO internal standard. RT = room temperature. *The kieserite sample initially contained 6 wt% hexahydrite; the displayed pattern had been acquired after 16 hr of heating, after all hexahydrite had become amorphous.

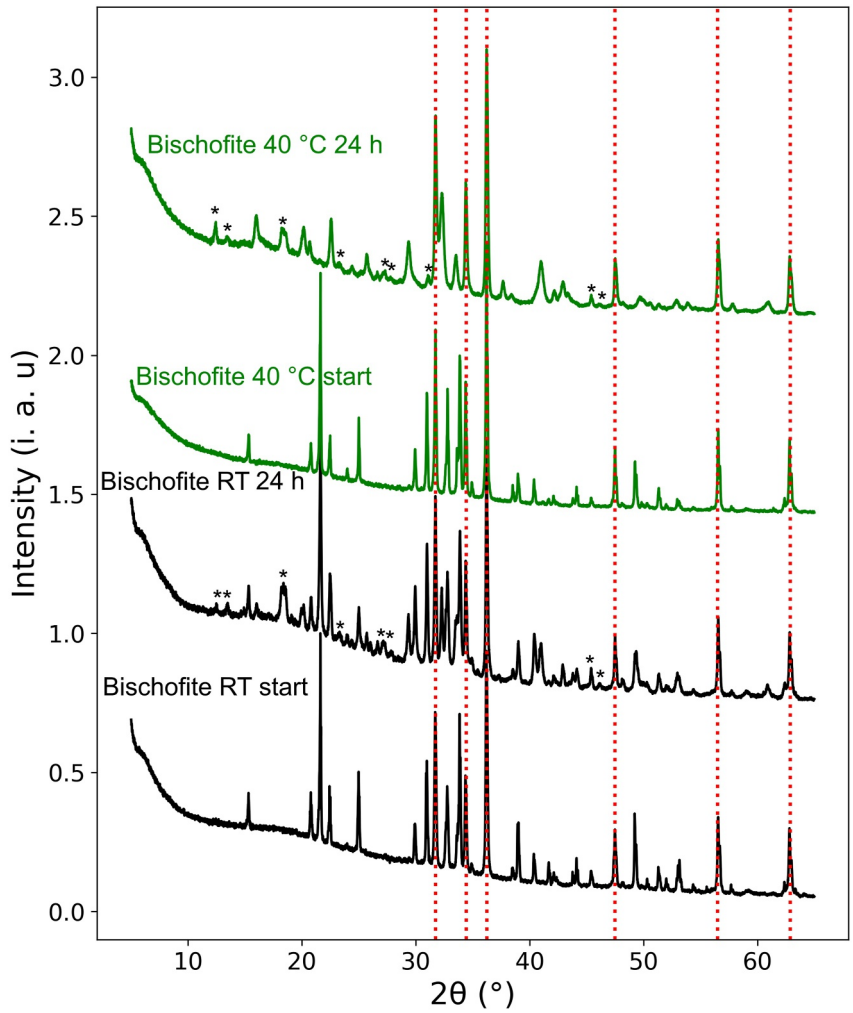

Figure 3. X-ray diffraction patterns acquired at the start and end of the individual runs for bischofite. Dotted vertical red lines mark Bragg peaks originating from the ZnO internal standard. RT = room temperature. *marks Bragg peaks stemming from the unknown $MgCl_2$ phase.

Experimental studies on starkeyite ($MgSO_4 \cdot 4H_2O$) report conflicting results, and there appears to be no consensus in the literature, with Chipera and Vaniman (2007) recording starkeyite's transformation to amorphous sulfate under vacuum, whereas Wang et al. (2006) find it to be stable under comparable conditions. In this study, starkeyite showed no signs of amorphization when stored at an uncontrolled room temperature of 20–21°C under CheMin-like conditions. This result was unexpected, as this temperature is approximately 5°C higher than the average internal temperature of the CheMin instrument (Vaniman et al., 2018), suggesting that starkeyite amorphization likely proceeds only during the diurnal temperature peaks. To test this hypothesis, starkeyite was also exposed to 40°C under CheMin-like conditions (Mars pressure at 0% RH) and indeed had partially amorphized after 24 hr (Table 1). Notably, the CheMin team reduced the residence time of the drill sample inside the instrument prior to the start of the analysis from ∼8 hr at Canaima to ∼4 hr at Ubajara. This shorter residence time may have contributed to the higher abundance of starkeyite observed at Ubajara (6.4 wt%) compared to Canaima (2.3 wt%).

In the 55 wt% kieserite and 4 wt% hexahydrite mixture, hexahydrite turned completely amorphous after 16 hr at 40°C. However, heating the sample for another 24 hr at 40°C did not result in any further amorphization, in line with kieserite's stability inside CheMin during several nights of subsequent analysis on Mars (Tutolo et al., 2025). These results are in agreement with previous reports on the high stability of kieserite under high-vacuum and dry

conditions at room temperature (Chipera & Vaniman, 2007; Vaniman et al., 2004) and further demonstrate that this stability field extends to higher temperatures.

3.2.2. $FeSO_4$–H_2O System

The stability of melanterite, rozenite, and szomolnokite under CheMin-like conditions showed behavior broadly analogous to that of the $MgSO_4$ hydrates, with the higher hydrates being less stable than the lower ones (Figure 2). Melanterite completely transformed to amorphous material within 4 hr at 20°C, corresponding to the maximum ground temperature measured by Curiosity over the first 2500 mission sols (Martínez et al., 2021), indicating that like epsomite and hexahydrite, it is likely not stable under the desiccating and warm conditions prevailing at Gale crater at noon.

Rozenite is less stable than starkeyite, revealing signs of amorphization at 21°C, and almost complete amorphization after 24 hr at 40°C. The experimental temperatures of 21°C and 40°C approximate peak temperatures on ground and inside the rover rather well; thus, it seems plausible that the low stability of the ferrous sulfates under such conditions explains their absence in the CheMin data to date, although the SAM instrument suggests ferrous sulfate presence in several drilled samples (Clark et al., 2024). Regarding our earlier work, we would like to point out that while previous reports (Chio et al., 2007) on polymorphic phase transitions in rozenite at Mars-like temperatures are in error (Meusburger et al., 2023), our results suggest that rozenite is unlikely to survive the desiccating low-pressure conditions prevailing in the equatorial region of Mars at noon and is anticipated to turn X-ray amorphous.

Szomolnokite demonstrated excellent stability, with no observable amorphization even after 24 hr of exposure to the simulated low-pressure, low-humidity environment and 40°C, in line with its detection in many orbital studies (e.g., Bishop et al., 2025). Overall, the data from both the $FeSO_4$-H_2O and $MgSO_4$-H_2O systems confirm a general trend: highly hydrated sulfate minerals are increasingly susceptible to amorphization under CheMin-like conditions.

3.2.3. Bischofite ($MgCl_2 \cdot 6H_2O$)

After observing a trend of increasing susceptibility to amorphization with hydration state in the $FeSO_4$ and $MgSO_4$ systems, it was natural to see if this behavior extends to other hydrated salts. The mineral bischofite ($MgCl_2 \cdot 6H_2O$) was chosen, since in terrestrial oceanic salt deposits it often co-occurs with the mineral kieserite (Czapowski et al., 2022), which has now been identified at three different drill locations by Curiosity, as well at numerous other locations in the equatorial region of Mars from orbit (Roach et al., 2009; Sheppard et al., 2021; Tutolo et al., 2025). Furthermore, moderate chlorine content (~4–7 wt.%) is observed in some kieserite-bearing rocks in Gale crater (O'Connell-Cooper et al., 2025). Bischofite has extremely high solubility and is often used as an indicator for low water activity brines ($a_w < 0.32$; (Ha & Chan, 1999)). Geochemical modeling suggests that the formation temperature of kieserite and anhydrite may be reduced under low-water activity conditions (Tosca et al., 2011). Therefore, bischofite's presence or absence has implications for the locus and conditions of kieserite formation on Mars. Our experiments aimed to determine if bischofite could turn amorphous under CheMin-like conditions. If not, then bischofite is truly absent (within the limit of detections) in the kieserite and anhydrite-bearing samples from Gale crater.

Our experimental results suggest that bischofite does not become amorphous at ~20°C or 40°C. Instead, it partially dehydrates to $MgCl_2 \cdot 4H_2O$ and a previously unknown phase (Figure 3). Notably, bischofite dehydration remained incomplete even after 24 hr at 40°C, highlighting the sluggishness of the reaction. Since neither, $MgCl_2 \cdot 4H_2O$, nor the unknown phase (with diffraction peaks located at 7.10, 6.56, 4.78, 4.58, 3.42, 3.33, 3.27, 3.22, 2.00 Å) have been detected by CheMin, we conclude that bischofite is truly absent in the kieserite-bearing drill samples at Gale crater - at least within the detection limits of the CheMin instrument. Interestingly, $MgCl_2 \cdot 6H_2O$ was previously thought to dehydrate to $MgCl_2 \cdot 4H_2O$ only above 69°C (Huang et al., 2011), thus $MgCl_2 \cdot 4H_2O$ had not been considered a plausible mineral candidate at Gale crater. A systematic investigation into the dependency of its dehydration temperature on experimental parameters (air pressure, $p(H_2O)$, and heating rate) is a worthwhile research endeavor, in particular since $MgCl_2 \cdot 6H_2O$ is a promising high-energy storage material (Ferchaud et al., 2012). Further investigations should also explore whether the formation of $MgCl_2 \cdot 4H_2O$ and the unknown phase can proceed under even colder, yet equally dry Martian surface conditions-such as those prevailing at noon, as it may be a promising candidate for a previously unrecognized Martian mineral. The Raman and infrared spectra for various

phases in the $MgCl_2$–H_2O, including the tetrahydrate, are reported by Shi et al. (2019), while the crystallographic information file for $MgCl_2 \cdot 4H_2O$ is reported by Schmidt et al. (2012) and may aid its identification by CRISM, SHERLOC or CheMin.

Comparing the stability of bischofite in CheMin-like conditions with the $FeSO_4$–H_2O, and $MgSO_4$–H_2O systems, it is noteworthy that bischofite (wt% (H_2O) = 53.2) is more hydrated than either epsomite (wt% (H_2O) = 51.2) or melanterite (wt% (H_2O) = 45.4), indicating that amorphization is not a straightforward function of water content. Systematic studies across a wider range of mineral systems (e.g., chlorides, sulfates, phosphates, and mixed compounds) might reveal the underlying reason for the different response of hydrated salts to desiccating conditions.

3.2.4. Amorphization on Ground Versus Inside CheMin

The observed susceptibility of higher sulfate hydrates to amorphization raises the question of what is the natural state of sulfate hydrates in bedrock at the Martian surface and what degree of change occurred inside the rover after sample delivery. Our laboratory studies show that epsomite, hexahydrite, and melanterite dehydrate rapidly (within <7 hr) at 20°C—corresponding to the peak midday temperatures recorded at Gale crater (Martínez et al., 2021). This suggests that these phases are inherently unstable under current surface conditions prevailing in the equatorial region and would likely have undergone amorphization during warm midday periods rather than inside the CheMin instrument. Once formed, the resulting amorphous Mg-sulfate phase appears stable under the cold and relatively humid nighttime conditions at Gale, likely preventing recrystallization (Vaniman & Chipera, 2006).

Perseverance's SHERLOC Raman instrument can identify minerals directly on the ground, enabling analysis of the hydration states of various salt hydrates in equilibrium with the present-day Martian atmosphere, the results of which are likely transferable to Gale crater. Analysis of several hundred sulfate mineral detections by SHERLOC at Jezero crater indicates that higher hydrates are rare in the equatorial region, with pentahydrite ($MgSO_4 \cdot 5H_2O$) representing the highest observed hydration state in the $MgSO_4$–H_2O system and the vast majority of sulfate hydrate detections being clustered in the mid- to low-hydration state region (Phua et al., 2024). This lends further support to the hypothesis that highly-hydrated minerals that are most likely to turn amorphous inside CheMin are rare in the equatorial region of Mars, and much of the salt-associated amorphous component (e.g., up to 24 wt % amorphous $MgSO_4$ at the Canaima drill site (Chipera et al., 2023; Simpson et al., 2025) was already amorphous on the surface before delivery into CheMin.

3.3. Extent of the Effect for Future Landed Missions

Several minerals and mineral candidates relevant to the Martian surface have thermal stability limits lower than the maximum temperature inside the MSL, thus preventing their detection (Table 2). However, many of these phases are also thermally unstable at the highest surface temperatures in the equatorial region, suggesting that they cannot persist under the desiccating and comparatively warm conditions prevailing at Gale crater at noon and early afternoon (i.e., 20°C). Moreover, their formation under the colder, more humid nighttime conditions is slow, making their presence at Gale crater unlikely, even on a transient basis (Vaniman et al., 2025).

Other future mission concepts such as the Rosalind Franklin rover and the Mars Life Explorer, however, propose to drill deeper, several meters into the subsurface, and extract and analyze mineral samples. The Mars Life Explorer, in particular, would likely drill into icy regolith in its search for extant life (Williams et al., 2023). At Gale crater, below the diurnal skin depth (~30 cm), minerals are in general exposed to temperatures of ~−48 and ~−58°C in summer and winter, respectively (Martínez et al., 2021). Several minerals may occur under such conditions that are unstable both when brought to the surface and even more so when transferred into the body of a spacecraft. The response of potential biosignatures to resulting mineral transformations is largely unexplored; however, it is likely that the large volume collapse often associated with dehydration and amorphization reaction that will have a negative effect on biomarker preservation. Vaniman and Chipera (2006) demonstrated that lower-hydrates, like kieserite, will hydrate in the presence of water ice over geological timescales, even at low-temperatures. Several other cryohydrates could form in a similar manner and are known from laboratory studies (Table 2).

The thermal stabilities of many compounds listed in Table 2 strongly depend on RH (Chipera & Vaniman, 2007; Chou et al., 2002). Based on these observations, temperature and humidity need to be controlled, or at least

Table 2
Selected Crystalline Phases With Thermal Stability Below the Maximum Temperature Recorded Inside the Curiosity Rover (i.e., 35°C)

Mineral	Stoichiometry	Upper limit of thermal stability (°C)	Reference
Ice Ih	H_2O	0	Fortes (2018)
Dry ice	CO_2	−78	Lide (2004)
meridaniite	$MgSO_4 \cdot 11H_2O$	2	Peterson et al. (2007)
ikaite	$CaCO_3 \cdot 6H_2O$	7	Huggett et al. (2005)
hydrohalite	$NaCl \cdot 2H_2O$	0	Light et al. (2009)
bischofite	$MgCl_2 \cdot 6\ H_2O$	20	This study
epsomite	$MgSO_4 \cdot 7H_2O$	20	This study, (Vaniman et al., 2004)
melanterite	$FeSO_4 \cdot 7H_2O$	20	This study
gypsum	$CaSO_4 \cdot 2H_2O$	ND	Vaniman et al. (2018)
chalcanithite	$CuSO_4 \cdot 5H_2O$	21	Chou et al. (2002)
synthetic	$NaCl \cdot 8.5H_2O$	−33	Journaux et al. (2023)
synthetic	$MgSO_4 \cdot 9H_2O$	−23	Fortes et al. (2017)
synthetic	$Na_2SO_4 \cdot 7H_2O$	10	Hall and Hamilton (2008)
synthetic	$MgCl_2 \cdot 12H_2O$	−8	Hennings et al. (2013)
synthetic	$MgCl_2 \cdot 8H_2O$	−3	Hennings et al. (2013)
synthetic	$MgCO_3 \cdot 6H_2O$	20	Rincke et al. (2020)
synthetic	$NiSO_4 \cdot 9\ H_2O$	−28 to −23	Fortes et al. (2018)
synthetic	$NiSO_4 \cdot 8\ H_2O$	0	Fortes et al. (2018)

Note. Some have been identified as natural minerals, while others are hitherto only known as synthetic compounds but may occur as minerals in the Martian subsurface. ND = upper stability temperature not determined but observed to dehydrate inside CheMin.

monitored, both during sampling as well as during analysis inside spacecraft if missions aim to analyze the pristine, unaltered subsurface mineralogy. Such cryosampling and analysis will likely also have a beneficial effect on biomarker preservation and may therefore not only be a requirement from a mineralogical perspective but also for the fidelity of life-detection instruments on future missions. Cryosampling while drilling into ice-cemented regolith on future missions such as the Rosalind Franklin rover and the Mars Life Explorer could present a challenge to hydrated mineral identification. Drilling could induce heat that may melt water ice and subsequently dissolve water-soluble phases, thereby precluding their delivery to mineralogical instruments like an XRD. Developing drilling and sampling techniques that minimize phase changes will be an important area of technology development in the next few years.

In the absence of measurements under controlled temperature and RH, reducing the time for mineralogical analysis could also provide information on the as-sampled mineral assemblage. CheMinX is a next-generation XRD/XRF instrument in development that would provide mineralogical and geochemical information faster and using less power than MSL-CheMin (Rampe et al., 2021). Instead of an energy-sensitive CCD, CheMinX uses two different detectors that are each optimized for diffraction and fluorescence. A hybrid-pixel array provides diffraction data without the need for active cooling, and a silicon drift detector provides X-ray fluorescence data. An X-ray focusing optic on CheMinX would produce XRD patterns in a matter of minutes compared to the many hours of analysis required by MSL - CheMin. Because diffraction data are collected in a few minutes, hydrated phases that are sensitive to changes in RH and temperature may not have time to transform before or during analysis. For MSL - CheMin, efforts to optimize the sample-acquisition workflow - particularly by reducing the time the sample resides inside the instrument before analysis - also help preserve the pristine mineralogy of the target rock.

Regarding the ExoMars mission, it is noteworthy that the relatively high temperatures inside the MSL rover originate from the heat emitted by the RTG, while the Rosalind Franklin rover uses solar panels to generate

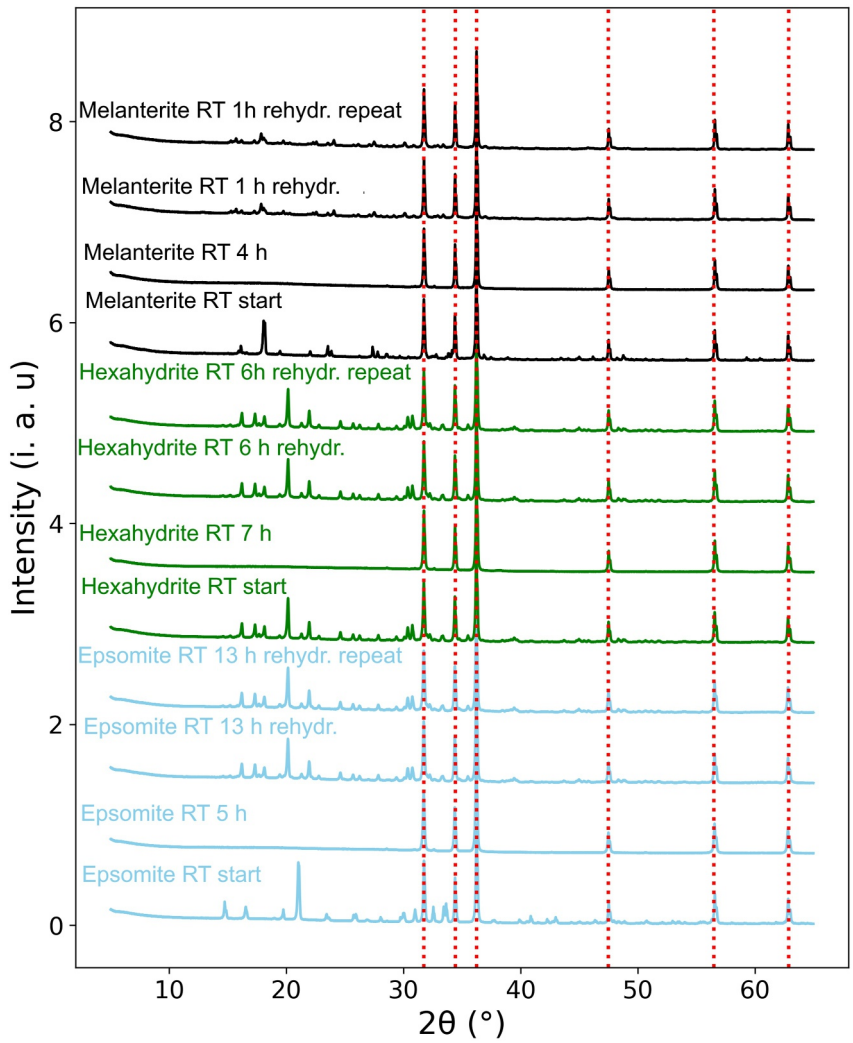

Figure 4. Recrystallization of amorphous magnesium sulfate hydrate and iron sulfate hydrate at Mars-relevant pressure and room temperature. Dotted vertical red lines mark Bragg peaks originating from the ZnO internal standard. RT = room temperature.

electricity, and temperatures inside the Analytical Laboratory Drawer are therefore estimated to remain much lower (typically −35° to −20°C). Under these conditions, many of the cryohydrates listed in Table 2 are stable. Even for extremely temperature- and moisture-sensitive samples, the rover's MicrOmega instrument can acquire infrared spectra in 15–25 min (Bibring et al., 2017; Loizeau et al., 2020). In addition, the nominal mission plan is to have a MicrOmega cube acquired on the same sol as the internal processing of the sample in the rover (including crushing, dosing, and flattening) such that the sample is not expected to sit in the rover for a protracted period before being analyzed, which further minimizes the risk for rover-induced mineral transformations and also allows the mineralogical evolution of the sample to be monitored inside the rover.

3.4. Opportunities for Future Landed Missions

Lastly, we consider the potential benefits of spaceflight instruments incorporating humidity and temperature control. We have found that increasing the humidity at CheMin-like pressure and temperatures leads to the crystallization of both amorphous $MgSO_4$ and $FeSO_4$ hydrates (Figure 4). The wt% of tracer ZnO in the recrystallized $MgSO_4$ samples agreed within 1.5 wt% with the values of the starting hexahydrite and epsomite samples, thus suggesting that the sample had fully recrystallized after seven (hexahydrite start) and 13 (epsomite start) hours. The XRD measurements were repeated to confirm that the sample indeed crystallized inside the

vacuum chamber and not during the measurement as indicated by essentially identical ZnO wt% derived from both measurements.

The amorphous $FeSO_4$ sample produced earlier in the melanterite run was exposed for only 1 hour to low-pressure, high-humidity conditions, and had almost completely (~90%) recrystallized (Figure 4), as derived by a comparison of the ZnO abundancies of the starting melanterite sample and the recrystallized sample. Again, the measurement was repeated to demonstrate that rehydration did not occur during the measurement. While the $MgSO_4$ samples were all rehydrated to phase-pure hexahydrite, the $FeSO_4$ was a complex phase mixture of melanterite (wt% = 8.8), siderotil ($FeSO_4 \cdot 5H_2O$; wt% = 24.7) and rozenite (wt% = 8.1). In particular, the formation of siderotil was unexpected since it had been previously thought that siderotil only forms via dehydration of copper-bearing melanterite (Jambor & Traill, 1963; Peterson et al., 2003).

The rapid recrystallization of both amorphous $MgSO_4$ and $FeSO_4$ hydrate suggests that raising the humidity inside the analysis chamber could induce the crystallization of salt-associated amorphous component, which accounts for up to 23 wt% of the drill samples (Chipera et al., 2023; Simpson et al., 2025), thus enabling their identification and quantification by CheMin. One of the main challenges in identifying trace phases in CheMin is the often relatively high overlap of Bragg peaks stemming from the ~6–10 phases typically observed in diffraction patterns from Gale crater. Hydration state changes induced by a controlled RH conditions inside a next-generation X-ray diffractometer would enable the monitoring of the disappearance of Bragg peaks and the emergence of new ones, thereby placing additional constraints on the identity of trace phases and X-ray amorphous materials.

For the implementation of such a cell, it is important to note that liquid water is unstable in the equatorial regions of Mars and will vaporize instantaneously upon exposure to the low-pressure atmosphere. Consequently, simply introducing small water drops into an analysis chamber would rapidly increase the humidity. No more than 173 mg of water would be sufficient to raise the RH of a 10-L reaction chamber at a temperature of 20°C to 100%. A strategic approach may involve introducing smaller water drops incrementally and collecting diffraction patterns between each addition. This would enable monitoring of the sample's mineralogical and crystallographic evolution as a function of RH. In addition, the CheMin sample chamber is in direct communication with the Martian atmosphere; thus, it appears beneficial to implement a lock system in a future instrument to seal off the sample chamber and prevent the escape of moisture. While the exact water usage of such a system depends on sample's uptake of atmospheric moisture, which reduces the RH inside the analysis chamber, we estimate that of the order of 10 mL of water would be sufficient for controlled humidity experiments on dozens of samples.

Such an approach would also be beneficial for the analysis of clay minerals, as unit-cell expansion or contraction in response to changing humidity conditions is a well-documented phenomenon (Kühnel & Van Der Gaast, 2005). These structural changes are most pronounced in the shift of the diagnostic basal reflection of phyllosilicates as well as several other Bragg peaks. A systematic investigation into the swelling behavior of various clay minerals under Martian pressure conditions as a function of humidity could provide valuable insights into the specific clay mineral species present. This information is particularly important, as both clays and salts play key roles in biomarker preservation and serve as paleoenvironmental indicators. Their presence and hydration state can yield critical constraints on past fluid temperature and chemistry (e.g., (Rampe et al., 2025) two essential parameters in evaluating the habitability of ancient Martian environments.

4. Conclusion

We have analyzed the temperature conditions inside the CheMin instrument over the first 45 sample acquisition campaigns (to sol 4266). Based on this data, we have investigated the stability of several hydrated minerals under simulated dry and warm conditions representative of the CheMin instrument. These experiments uncovered a hitherto undescribed $MgCl_2$ hydrate, which may form under present-day Mars environmental conditions. Efforts to further investigate the structure and properties of this phase are underway. In addition, we have synthesized pure copper-free siderotil for the first time. We further find that while highly hydrated minerals are more prone to transform inside the rover than the lower hydrates, the tendency of amorphization is not a straightforward function of the mineral's water content. The rapid amorphization of several salt hydrates at the maximum temperature recorded at Gale crater suggests that the amorphous salt-associated components were likely already amorphous on ground during sampling rather than forming inside the rover. While amorphization inside CheMin may therefore only make minimal contributions to the abundant salt-associated amorphous component detected in Gale crater samples, future landed missions are set to sample the deeper, colder Martian subsurface where highly hydrated,

thermally sensitive minerals may be present. In addition, we found that the salt-associated amorphous component may be rapidly crystallized by simply raising the RH inside the analysis chamber.

These findings suggest that to enable non-destructive mineral analysis for future landed missions, maintaining controlled temperature and RH conditions is essential and would significantly enhance analytical capabilities.

Conflict of Interest

The authors declare no conflicts of interest relevant to this study.

Data Availability Statement

All XRD and CheMin thermal data are archived in the Astrobiology Habitable Environments Database repository (Meusburger & Bristow, 2026).

Acknowledgments
JMM's research was supported by an appointment to the NASA Postdoctoral Program in the Exobiology Branch at the Ames Research Center, administered by Oak Ridge Associated Universities under contract with NASA.

References

Anderson, R. C., Jandura, L., Okon, A. B., Sunshine, D., Roumeliotis, C., Beegle, L. W., et al. (2012). Collecting samples in gale crater, Mars: An overview of the Mars science laboratory sample acquisition, sample processing and handling system. *Space Science Reviews*, *170*(1), 57–75. https://doi.org/10.1007/s11214-012-9898-9

Bibring, J.-P., Hamm, V., Pilorget, C., & Vago, J., & The MicrOmega Team. (2017). The MicrOmega investigation onboard ExoMars. *Astrobiology*, *17*(6–7), 621–626. https://doi.org/10.1089/ast.2016.1642

Bishop, J. L., Meusburger, J. M., Weitz, C. M., Parente, M., Gross, C., Talla, D., et al. (2025). Characterization of ferric hydroxysulfate on Mars and implications of the geochemical environment supporting its formation. *Nature Communications*, *16*(1), 7020. https://doi.org/10.1038/s41467-025-61801-2

Blake, D., Tu, V., Bristow, T., Rampe, E., Vaniman, D., Chipera, S., et al. (2024). The chemistry and mineralogy (CheMin) X-ray diffractometer on the MSL curiosity rover: A decade of mineralogy from gale crater, Mars. *Minerals*, *14*(6), 568. https://doi.org/10.3390/min14060568

Blake, D., Vaniman, D., Achilles, C., Anderson, R., Bish, D., Bristow, T., et al. (2012). Characterization and calibration of the CheMin mineralogical instrument on Mars science laboratory. *Space Science Reviews*, *170*(1), 341–399. https://doi.org/10.1007/s11214-012-9905-1

Bristow, T. F., Bish, D. L., Vaniman, D. T., Morris, R. V., Blake, D. F., Grotzinger, J. P., et al. (2015). The origin and implications of clay minerals from Yellowknife Bay, Gale crater, Mars. *American Mineralogist*, *100*(4), 824–836. https://doi.org/10.2138/am-2015-5077CCBYNCND

Bristow, T. F., Grotzinger, J. P., Rampe, E. B., Cuadros, J., Chipera, S. J., Downs, G. W., et al. (2021). Brine-driven destruction of clay minerals in Gale crater, Mars. *Science*, *373*(6551), 204. https://doi.org/10.1126/science.abg5449

Carter, J., Riu, L., Poulet, F., Bibring, J.-P., Langevin, Y., & Gondet, B. (2023). A Mars orbital catalog of aqueous alteration signatures (MOCAAS). *Icarus*, *389*, 115164. https://doi.org/10.1016/j.icarus.2022.115164

Chio, C., Sharma, S., & Muenow, D. (2007). The hydrates and deuterates of ferrous sulfate ($FeSO_4$): A Raman spectroscopic study. *Journal of Raman Spectroscopy*, *38*(1), 87–99. https://doi.org/10.1002/jrs.1623

Chipera, S. J., & Vaniman, D. T. (2007). Experimental stability of magnesium sulfate hydrates that may be present on Mars. *Geochimica et Cosmochimica Acta*, *71*(1), 241–250. https://doi.org/10.1016/j.gca.2006.07.044

Chipera, S. J., Vaniman, D. T., Rampe, E. B., Bristow, T. F., Martínez, G., Tu, V. M., et al. (2023). Mineralogical investigation of Mg-Sulfate at the Canaima drill site, gale crater, Mars. *Journal of Geophysical Research: Planets*, *128*(11), e2023JE008041. https://doi.org/10.1029/2023JE008041

Chou, I.-M., Seal, R. R., & Hemingway, B. S. (2002). Determination of melanterite-rozenite and chalcanthite-bonattite equilibria by humidity measurements at 0.1 MPa. *American Mineralogist*, *87*(1), 108–114. https://doi.org/10.2138/am-2002-0112

Christensen, P. R., Wyatt, M. B., Glotch, T. D., Rogers, A. D., Anwar, S., Arvidson, R. E., et al. (2004). Mineralogy at Meridiani Planum from the Mini-TES experiment on the opportunity rover. *Science*, *306*(5702), 1739. https://doi.org/10.1126/science.1104909

Clark, J. V., Sutter, B., McAdam, A. C., Lewis, J. M. T., Franz, H., Archer, P. D., et al. (2024). Environmental changes recorded in sedimentary rocks in the clay-sulfate transition Region in gale crater, Mars: Results from the sample analysis at mars-evolved gas analysis instrument onboard the Mars science laboratory curiosity rover. *Journal of Geophysical Research: Planets*, *129*(12), e2024JE008587. https://doi.org/10.1029/2024JE008587

Czapowski, G., Tomassi-Morawiec, H., Handke, B., Wachowiak, J., & Peryt, T. (2022). Trace elements and mineralogy of Upper Permian (Zechstein) potash deposits in Poland. *Applied Sciences*, *12*(14), 7183. https://doi.org/10.3390/app12147183

Ferchaud, C., Zondag, H., Veldhuis, J., & Boer, R. (2012). Study of the reversible water vapour sorption process of $MgSO_4.7H_2O$ and $MgCl_2.6H_2O$ under the conditions of seasonal solar heat storage. *Journal of Physics: Conference Series*, *395*(1), 12069. https://doi.org/10.1088/1742-6596/395/1/012069

Fortes, A. D. (2018). Accurate and precise lattice parameters of H_2O and D_2O ice I h between 1.6 and 270K from high-resolution time-of-flight neutron powder diffraction data. *Acta Crystallographica Section B*, *74*(2), 196–216. https://doi.org/10.1107/S2052520618002159

Fortes, A. D., Knight, K. S., Gibbs, A. S., & Wood, I. G. (2018). Crystal structures of $NiSO_4{\cdot}9H_2O$ and $NiSO_4{\cdot}8H_2O$: Magnetic properties, stability with respect to morenosite ($NiSO_4{\cdot}7H_2O$), the solid-solution series $(Mg_xNi_{1-x})SO_4{\cdot}9H_2O$. *Physics and Chemistry of Minerals*, *45*(8), 695–712. https://doi.org/10.1007/s00269-018-0956-z

Fortes, A. D., Knight, K. S., & Wood, I. G. (2017). Structure, thermal expansion and incompressibility of $MgSO_4{\cdot}9H_2O$, its relationship to meridianiite ($MgSO_4{\cdot}11H_2O$) and possible natural occurrences. *Acta Crystallographica Section B*, *73*(1), 47–64. https://doi.org/10.1107/S2052520616018266

Furnari, F., Piccioni, G., DeAngelis, S., Stefani, S., Tosi, F., Carli, C., et al. (2025). Infrared reflectance spectra of Hexahydrite at typical Jupiter's icy moons environmental conditions. *EGU General Assembly*. https://doi.org/10.5194/egusphere-egu25-11300

Greenspan, L. (1977). Humidity fixed points of binary saturated aqueous solutions. *Journal of Research of the National Bureau of Standards. Section A. Physics and Chemistry*, *81A*(1), 89–96. https://doi.org/10.6028/jres.081a.011

Ha, H., & Chan, C. (1999). The water activities of $MgCl_2$, $Mg(NO_3)_2$, $MgSO_4$, and their mixtures. *Aerosol Science & Technology*, *31*(2–3), 154–169. https://doi.org/10.1080/027868299304219

Hall, C., & Hamilton, A. (2008). The heptahydrate of sodium sulfate: Does it have a role in terrestrial and planetary geochemistry? *Icarus*, *198*(1), 277–279. https://doi.org/10.1016/j.icarus.2008.07.001

Hennings, E., Schmidt, H., & Voigt, W. (2013). Crystal structures of hydrates of simple inorganic salts. I. Water-rich magnesium halide hydrates $MgCl_2{\cdot}8H_2O$, $MgCl_2{\cdot}12H_2O$, $MgBr_2{\cdot}6H_2O$, $MgBr_2{\cdot}9H_2O$, $MgI_2{\cdot}8H_2O$ and $MgI_2{\cdot}9H_2O$. *Acta Crystallographica Section C*, *69*(11), 1292–1300. https://doi.org/10.1107/S0108270113028138

Hillier, S. (2000). Accurate quantitative analysis of clay and other minerals in sandstones by XRD: Comparison of a Rietveld and a reference intensity ratio (RIR) method and the importance of sample preparation. *Clay Minerals*, *35*(1), 291–302. https://doi.org/10.1180/000985500546666

Huang, Q., Lu, G., Wang, J., & Yu, J. (2011). Thermal decomposition mechanisms of $MgCl_2{\cdot}6H_2O$ and $MgCl_2{\cdot}H_2O$. *Journal of Analytical and Applied Pyrolysis*, *91*(1), 159–164. https://doi.org/10.1016/j.jaap.2011.02.005

Huggett, J. M., Schultz, B. P., Shearman, D. J., & Smith, A. J. (2005). The petrology of ikaite pseudomorphs and their diagenesis. *Commemorating the Life and Work of Douglas Shearman, 1918–2003*, *116*(3), 207–220. https://doi.org/10.1016/S0016-7878(05)80042-2

Jambor, J. L., & Traill, R. J. (1963). On rozenite and siderotil. *The Canadian Mineralogist*, *7*(5).

Journaux, B., Pakhomova, A., Collings, I. E., Petitgirard, S., Boffa Ballaran, T., Brown, J. M., et al. (2023). On the identification of hyperhydrated sodium chloride hydrates, stable at icy moon conditions. *Proceedings of the National Academy of Sciences*, *120*(9), e2217125120. https://doi.org/10.1073/pnas.2217125120

Karsten, O. (1954). Lösungsgeschwindigkeit von Natriumchlorid, Kaliumchlorid und Kieserit in Wasser und in wässerigen Lösungen. *Zeitschrift für Anorganische und Allgemeine Chemie*, *276*(5–6), 247–266. https://doi.org/10.1002/zaac.19542760506

Kühnel, R. A., & Van Der Gaast, S. J. (2005). XRD of wet specimen – Source of interesting information. *Acta Geodynamica et Geomaterialia*, *2*(138), 95–104.

Lide, D. R. (Ed.) (2004)., *CRC handbook of chemistry and physics* (85th ed.). CRC Press.

Light, B., Brandt, R. E., & Warren, S. G. (2009). Hydrohalite in cold sea ice: Laboratory observations of single crystals, surface accumulations, and migration rates under a temperature gradient, with application to "Snowball Earth". *Journal of Geophysical Research*, *114*(C7). https://doi.org/10.1029/2008JC005211

Loizeau, D., Lequertier, G., Poulet, F., Hamm, V., Pilorget, C., Meslier-Lourit, L., et al. (2020). Planetary Terrestrial Analogues Library project: 2. Building a laboratory facility for MicrOmega characterization. *Planetary and Space Science*, *193*, 105087. https://doi.org/10.1016/j.pss.2020.105087

Martínez, G. M., Vicente-Retortillo, A., Vasavada, A. R., Newman, C. E., Fischer, E., Rennó, N. O., et al. (2021). The surface energy budget at Gale crater during the first 2500 sols of the Mars science laboratory Mission. *Journal of Geophysical Research: Planets*, *126*(9), e2020JE006804. https://doi.org/10.1029/2020JE006804

Meusburger, J. M., & Bristow, T. (2026). Data from: Rover-induced mineral transformations: Extent of the effect for the Mars Science Laboratory and opportunities for future landed missions [Dataset]. *Astrobiology Habitable Environment Database*. https://doi.org/10.48667/yhps-gp67

Meusburger, J. M., Ende, M., Matzinger, P., Talla, D., Miletich, R., & Wildner, M. (2020). Polymorphism of Mg-sulfate monohydrate kieserite under pressure and its occurrence on giant icy jovian satellites. *Icarus*, *336*, 113459. https://doi.org/10.1016/j.icarus.2019.113459

Meusburger, J. M., Ende, M., Talla, D., Wildner, M., & Miletich, R. (2019). Transformation mechanism of the pressure-induced C2/c-to-$P1^-$ transition in ferrous sulfate monohydrate single crystals. *Journal of Solid State Chemistry*, *277*, 240–252. https://doi.org/10.1016/j.jssc.2019.06.004

Meusburger, J. M., Hudson-Edwards, K. A., Tang, C. C., Connolly, E. T., Crane, R. A., & Fortes, A. D. (2023). Low-temperature crystallography and vibrational properties of rozenite ($FeSO_4{\cdot}4H_2O$), a candidate mineral component of the polyhydrated sulfate deposits on Mars. *American Mineralogist*, *108*(6), 1080–1091. https://doi.org/10.2138/am-2022-8502

Néri, A., Guyot, F., Reynard, B., & Sotin, C. (2020). A carbonaceous chondrite and cometary origin for icy moons of Jupiter and Saturn. *Earth and Planetary Science Letters*, *530*, 115920. https://doi.org/10.1016/j.epsl.2019.115920

O'Connell-Cooper, C., Spray, J., Gellert, R., Thompson, L., Berger, J., Boyd, N., et al. (2025). Salty Mars -NA enrichments associated with CL, S, mg, CA in the layered SUL- fate unit, Gale crater, MARS: Apxs identification and implications. https://doi.org/10.17189/1518757

Peterson, R. C., Nelson, W., Madu, B., & Shurvell, H. F. (2007). Meridianiite: A new mineral species observed on Earth and predicted to exist on Mars. *American Mineralogist*, *92*(10), 1756–1759. https://doi.org/10.2138/am.2007.2668

Peterson, R. C., Roeder, P., & Zhang, Y. (2003). The atomic structure of siderotil, (Fe, Cu)$SO_4{\cdot}5H_2O$. *The Canadian Mineralogist*, *41*.

Phua, Y. Y., Ehlmann, B. L., Siljeström, S., Czaja, A. D., Beck, P., Connell, S., et al. (2024). Characterizing hydrated sulfates and altered phases in jezero Crater fan and floor geologic units with SHERLOC on Mars 2020. *Journal of Geophysical Research: Planets*, *129*(7), e2023JE008251. https://doi.org/10.1029/2023JE008251

Rampe, E. B., Blake, D., Sarrazin, P., Bristow, T., Gailhanou, M., Lafuente, B., et al. (2021). CheMinX: A next generation XRD/XRF for quantitative mineralogy and geochemistry on Mars. *Bulletin of the AAS*, *53*(4). https://doi.org/10.3847/25c2cfeb.a4a55445

Rampe, E. B., Blake, D. F., Bristow, T. F., Ming, D. W., Vaniman, D. T., Morris, R. V., et al. (2020). Mineralogy and geochemistry of sedimentary rocks and eolian sediments in Gale crater, Mars: A review after six Earth years of exploration with Curiosity. *Geochemistry*, *80*(2), 125605. https://doi.org/10.1016/j.chemer.2020.125605

Rampe, E. B., Tu, V., Morris, R., Clark, J., Bristow, T., Ehlmann, B., et al. (2025). Evidence for partially chloritized smectite in Gale crater, Mars. *Clays and Clay Minerals*, *73*, e17. https://doi.org/10.1017/cmn.2024.42

Rincke, C., Schmidt, H., & Voigt, W. (2020). A new hydrate of magnesium carbonate, $MgCO_3{\cdot}6H_2O$. *Acta Crystallographica Section C*, *76*(3), 244–249. https://doi.org/10.1107/S2053229620001540

Roach, L. H., Mustard, J. F., Murchie, S. L., Bibring, J.-P., Forget, F., Lewis, K. W., et al. (2009). Testing evidence of recent hydration state change in sulfates on Mars. *Journal of Geophysical Research*, *114*(E2). https://doi.org/10.1029/2008JE003245

Royer, C., Bedford, C. C., Johnson, J. R., Horgan, B. H. N., Broz, A., Forni, O., et al. (2024). Intense alteration on early Mars revealed by high-aluminum rocks at Jezero crater. *Communications Earth & Environment*, *5*(1), 671. https://doi.org/10.1038/s43247-024-01837-2

Schmidt, H., Hennings, E., & Voigt, W. (2012). Magnesium chloride tetrahydrate, $MgCl_2{\cdot}4H_2O$. *Acta Crystallographica Section C*, *68*(1), i4–i6. https://doi.org/10.1107/S0108270111054709

Sheppard, R. Y., Milliken, R. E., Parente, M., & Itoh, Y. (2021). Updated perspectives and hypotheses on the mineralogy of lower Mt. Sharp, Mars, as seen from orbit. *Journal of Geophysical Research: Planets*, *126*(2), e2020JE006372. https://doi.org/10.1029/2020JE006372

Sheppard, R. Y., Milliken, R. E., & Robertson, K. M. (2022). Presence of clay minerals can obscure spectral evidence of Mg sulfates: Implications for orbital observations of Mars. *Icarus*, *383*, 115083. https://doi.org/10.1016/j.icarus.2022.115083

Shi, E., Ling, Z., & Wang, A. (2019). MIR, NIR and Raman Spectra of Magnesium chlorides with six hydration degrees – Implication for Mars and europa. *50th Lunar and Planetary Science Conference*, *2546*. https://www.hou.usra.edu/meetings/lpsc2019/pdf/2546.pdf

Siljeström, S., Czaja, A., Corpolongo, A., Berger, E., Li, A., Cardarelli, E., et al. (2024). Evidence of sulfate-rich fluid alteration in jezero Crater floor, Mars. *Journal of Geophysical Research: Planets*, *129*(1), e2023JE007989. https://doi.org/10.1029/2023JE007989

Simpson, S. L., VanBommel, S. J., Rampe, E. B., Bristow, T. F., Achilles, C., Morrison, S., et al. (2025). X-ray amorphous materials in gale crater, Mars: Observations, major trends and implications for paleoenvironmental conditions. *56th Lunar and Planetary Science Conference (LPSC)*.

Squyres, S. W., Arvidson, R. E., Ruff, S., Gellert, R., Morris, R. V., Ming, D. W., et al. (2008). Detection of Silica-Rich deposits on Mars. *Science*, *320*(5879), 1063–1067. https://doi.org/10.1126/science.1155429

Toby, B. H., & Von Dreele, R. B. (2013). GSAS-II: The genesis of a modern open-source all purpose crystallography software package. *Journal of Applied Crystallography*, *46*(2), 544–549. https://doi.org/10.1107/S0021889813003531

Tosca, N. J., McLennan, S. M., Lamb, M. P., & Grotzinger, J. P. (2011). Physicochemical properties of concentrated Martian surface waters. *Journal of Geophysical Research*, *116*(E5), Article E5. https://doi.org/10.1029/2010JE003700

Tutolo, B. M., Hausrath, E. M., Kite, E. S., Rampe, E. B., Bristow, T. F., Downs, R. T., et al. (2025). Carbonates identified by the Curiosity rover indicate a carbon cycle operated on ancient Mars. *Science*, *388*(6744), 292–297. https://doi.org/10.1126/science.ado9966

Vago, J. L., Westall, F., Pasteur Instrument Teams, L. S. S. W. G., Other, C., Coates, A. J., Jaumann, R., et al. (2017). Habitability on early Mars and the search for biosignatures with the ExoMars rover. *Astrobiology*, *17*(6–7), 471–510. https://doi.org/10.1089/ast.2016.1533

Vaniman, D., Chipera, S., Rampe, E., Bristow, T., Blake, D., Meusburger, J., et al. (2024). Gypsum on Mars: A detailed view at Gale crater. *Minerals*, *14*(8), 815. https://doi.org/10.3390/min14080815

Vaniman, D., Martínez, G., Chipera, S., Morris, R. V., Rampe, E., Bristow, T., et al. (2025). Meridianiite at Gale crater? In *56th Lunar and Planetary Science Conference*. Abstract number 1326.

Vaniman, D. T., Bish, D. L., Chipera, S. J., Fialips, C. I., William Carey, J., & Feldman, W. C. (2004). Magnesium sulphate salts and the history of water on Mars. *Nature*, *431*(7009), 663–665. https://doi.org/10.1038/nature02973

Vaniman, D. T., & Chipera, S. J. (2006). Transformations of Mg- and Ca-sulfate hydrates in Mars regolith. *American Mineralogist*, *91*(10), 1628–1642. https://doi.org/10.2138/am.2006.2092

Vaniman, D. T., Martínez, G. M., Rampe, E. B., Bristow, T. F., Blake, D. F., Yen, A. S., et al. (2018). Gypsum, bassanite, and anhydrite at Gale crater, Mars. *American Mineralogist*, *103*(7), 1011–1020. https://doi.org/10.2138/am-2018-6346

Wang, A., Freeman, J., Jolliff, B., & Arvidson, R. (2006). Conversion of crystalline $MgSO_4{\cdot}XH_2O$ to the hydrated amorphous Phase—A raman, NIR, and XRD Study. In *Lunar and Planetary Science XXXVII*, Abstract number 2168.

Wang, A., Freeman, J. J., & Jolliff, B. L. (2009). Phase transition pathways of the hydrates of magnesium sulfate in the temperature range 50°C to 5°C: Implication for sulfates on Mars. *Journal of Geophysical Research*, *114*(E4), Article E4. https://doi.org/10.1029/2008JE003266

Williams, A. J., Muirhead, B., Matousek, S. E., Brinckerhoff, W. B., Ehlmann, B. L., Jakosky, B. M., et al. (2023). The Mars life explorer Mission concept. *AGU Fall Meeting Abstracts*, *2023*, P44C-05.